Available online at www.sciencedirect.com
SCIENCE DIRECT®
Journal of Solid State Chemistry 177 (2004) 3045–3051
JOURNAL OF SOLID STATE CHEMISTRY
http://elsevier.com/locate/jssc

Vibrational spectra of the peroxotantalates $(NH_4)_3[Ta(O_2)_4]$, $K_3[Ta(O_2)_4]$, $Rb_3[Ta(O_2)_4]$ and $Cs_3[Ta(O_2)_4]$ and the crystal structure of $Rb_3[Ta(O_2)_4]$

G. Haxhillazi and H. Haeuseler*

Laboratorium für Anorganische Chemie der, Universität Siegen, Adolf-Reichwein-Str. 9, Postfach 101240, D-57068 Siegen, Germany

Received 17 February 2004; received in revised form 27 April 2004; accepted 5 May 2004

Available online 25 June 2004

Abstract

The compounds $(NH_4)_3[Ta(O_2)_4]$, $K_3[Ta(O_2)_4]$, $Rb_3[Ta(O_2)_4]$ and $Cs_3[Ta(O_2)_4]$ have been prepared and investigated by X-ray powder methods as well as Raman- and IR-spectroscopy. In the case of $Rb_3[Ta(O_2)_4]$ the structure has been solved from single crystal data. It is shown that all these compounds are isotypic and crystallize in the $K_3[Cr(O_2)_4]$ type (SG $I\bar{4}2m$, No. 121). The infrared- and Raman spectra (recorded on powdered samples) are discussed with respect to the internal vibrations of the peroxo-group and the dodecahedral $[Ta(O_2)_4]^{3-}$ ion. Symmetry coordinates for the $[Ta(O_2)_4]^{3-}$ ion are given from which the vibrational modes of the O–O stretching vibrations of the O_2^{2-} groups, the Ta–O stretching vibrations and the Ta–O bending vibrations are deduced.

Keywords: Peroxocomplex; Vibrational spectra; $Rb_3[Ta(O_2)_4]$; Structure analysis

1. Introduction

In 1905 Riesenfeld [1] discovered red peroxochromates with the unusual oxidation state +V of the chromium. Later, during his studies on the structure of the potassium peroxochromate $K_3[Cr(O_2)_4]$ Wilson [2] prepared a series of compounds in which the chromium is replaced by pentavalent niobium or tantalum and which he describes as isotypic to $K_3[Cr(O_2)_4]$. In the following time the structure of $K_3[Cr(O_2)_4]$ was reinvestigated by Stomberg and Brosset [3], Stomberg [4], Swalen and Ibers [5], Fischer et al. [6], Wood et al. [7], and Cage and Dalal [8]. According to these measurements $K_3[Cr(O_2)_4]$ crystallizes in the tetragonal space group $I\bar{4}2m$ in a structure type named after this compound.

Of the tantalates $A_3[Ta(O_2)_4]$ with A = K, Rb, Cs which are said to be isotypic to $K_3[Cr(O_2)_4]$ [2] only little information is found in the literature. The structure of $K_3[Ta(O_2)_4]$ has been solved on single crystals by Wehrum and Hoppe [9] confirming the isotypy to the $K_3[Cr(O_2)_4]$ type at least for this compound. $(NH_4)_3[Ta(O_2)_4]$ has been described by Selezneva and Nisel'son [10] and characterized by XRD but in this paper only *d*-values are given and there is no information on the structure of this compound. The knowledge on the vibrational spectra of all these compounds is very limited. Some work has been done by Griffith [11] and Griffith et al. [12] who report on an intense band at 807 cm^{-1} in the infrared spectrum of $K_3[Ta(O_2)_4]$ due to the O–O stretching vibration which is also reported by Jere et al. [13] with a slightly different value. For the same vibration Bogdanov et al. [14] report a much higher value (860 cm^{-1}) and for $Rb_3[Ta(O_2)_4]$ and $Cs_3[Ta(O_2)_4]$ they find 870 cm^{-1}.

As a systematic investigation of the vibrational properties of the peroxo-compounds of the $K_3[Cr(O_2)_4]$-type is missing in the literature, we started infrared and Raman studies of these compounds and reported already on the vibrational properties of the chromiumperoxocomplexes of ammonium, potassium

*Corresponding author. Fax: +49-271-740-2555.
E-mail address: haeuseler@chemie.uni-siegen.de (H. Haeuseler).

0022-4596/$ - see front matter © 2004 Elsevier Inc. All rights reserved.
doi:10.1016/j.jssc.2004.05.011

and rubidium [15]. In this paper we focus on the corresponding tantalum compounds.

2. Experimental

For the preparation of $(NH_4)_3[Ta(O_2)_4]$ 0.5 g $TaCl_5$ was dissolved in 10 mL of 30 wt% hydrogen peroxide. The solution was cooled to −4°C and first 3 mL of 25 wt% ammonia were added and then 5 mL ethanol. The white precipitate was filtered off under a vacuum and washed with ethanol and ether. The product was stored in an refrigerator under −4°C. Under these conditions the product is relatively stable. After a storage of 1 month no decomposition of the product could be observed by X-ray diffraction.

For the preparation of $K_3[Ta(O_2)_4]$ first a mixture of 0.6 g Ta_2O_5 with 2.0 g potassium carbonate was molten in an alumina crucible in a furnace for 1 h at 800°C. The resulting melt was only partly dissolvable in 30 mL of water. After filtering, the clear solution was cooled to −4°C and 5 mL of 30 wt% hydrogen peroxide was added dropwise under vigorous stirring. Then 10 mL ethanol cooled to −4°C were added to result in a white precipitate which was filtered off under a vacuum, washed with ethanol and dried with ether. The product was stored in an refrigerator.

For the preparation of $Rb_3[Ta(O_2)_4]$ a mixture of 0.6 g Ta_2O_5 and 2.0 g Rb_2CO_3 were molten in at 800°C for 2 h. The cooled melt was dissolved in water, filtered, the clear solution cooled to −4°C, and then treated dropwise with 5 mL of 30 wt% hydrogenperoxide under vigorous stirring. After the addition of 30 mL of cool ethanol a white precipitate appeared which was filtered off, washed with cool ethanol, dried with ether and stored in a refrigerator.

For the preparation of the single crystals of $Rb_3[Ta(O_2)_4]$ stirring was stopped after the addition of the hydrogenperoxide and only 15 mL ethanol were added. This solution was placed in an exsiccator over ethanol and stored for 10 days in a refrigerator when small shiny colorless crystals appeared which were separated by filtration, washed with ethanol and dried with ether.

For the preparation of $Cs_3[Ta(O_2)_4]$ the same procedure as described for the rubidium compound was used.

The microcrystalline products have been investigated by powder X-ray diffraction methods using the Cu$K\alpha_1$ radiation ($\lambda = 154.06$ pm) of a Siemens D5000 diffractometer equipped with a Ge-monochromator and a position sensitive detector Braun PSD-50M. The calculation of the lattice parameters and the theoretical diagrams were done with the program package Stoe WinXPow [16].

For the single crystal measurement on $Rb_3[Ta(O_2)_4]$ a Stoe Image Plate Diffraction System at room temperature was employed, which works with monochromatic (graphite monochromator) Mo$K\alpha$ radiation ($\lambda = 71.073$ pm). A colorless crystal with the dimension $0.42 \times 0.37 \times 0.20\,mm^3$ which had the form of a parallelepiped with prismatic ends was mounted on top of a glass capillary and was turned stepwise from $\varphi = -1°$ to 360° with an increment of $\varphi = 1°$. The structure was solved using the program Shelx [17].

The infrared spectra of the compounds have been measured at room temperature on powdered samples with a Bruker IFS 113 V spectrometer using KBr discs. The Raman spectra were recorded on a Bruker RFS 100/S spectrometer equipped with a Nd:YAG laser (excitation line: 1064 nm) on samples sealed in glass capillaries. The resolution of all the vibrational spectra was fixed to $2\,cm^{-1}$.

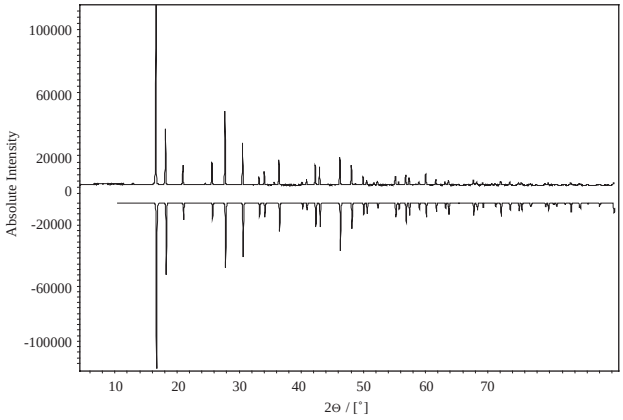

Fig. 1. X-ray powder diffraction pattern of $(NH_4)_3[Ta(O_2)_4]$ (top) in comparison to a pattern calculated on the basis of the fractional coordinates of $K_3[Ta(O_2)_4]$ [7] (bottom).

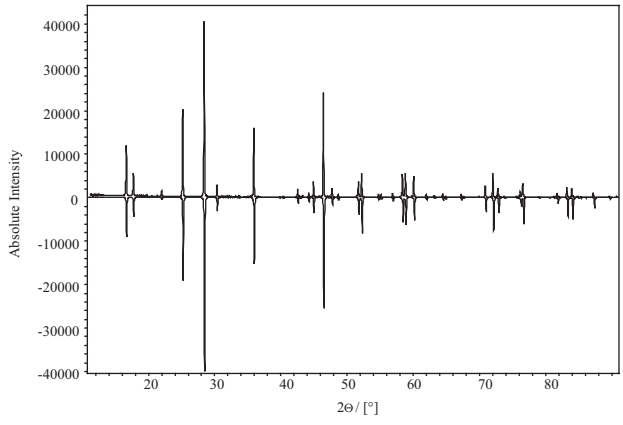

Fig. 2. X-ray powder diffraction pattern of $Rb_3[Ta(O_2)_4]$ (top) in comparison to a pattern calculated on the basis of the fractional coordinates of $K_3[Ta(O_2)_4]$ [7] (bottom).

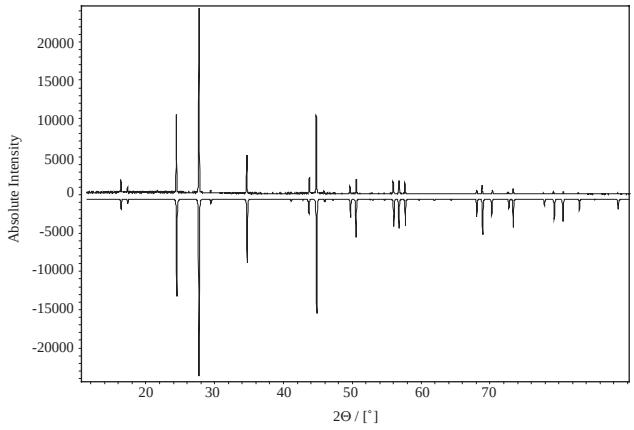

Fig. 3. X-ray powder diffraction pattern of $Cs_3[Ta(O_2)_4]$ (top) in comparison to a pattern calculated on the basis of the fractional coordinates of $K_3[Ta(O_2)_4]$ [7] (bottom).

Table 1
Experimental details of the crystal structure determination of $Rb_3[Ta(O_2)_4]$

Space group	$I\bar{4}2m$-D_{2d}^{11} (No. 121)
Crystal system	Tetragonal
Unit cell dimension (pm)	$a = 706.20(10)$, $c = 815.6(2)$
Volume (10^6 pm^3)	406.75(13)
Z (no. of molecules in the unit cell)	2
$F(000)$	496
Calculated density (Mg/m^3)	4.616
Linear absorption coefficient (mm^{-1})	31.351
Theta range θ (deg)	3.82–31.49
$h\,k\,l$ ranges	$-10 \leqslant h, \leqslant 10, -10 \leqslant k \leqslant 8, -11 \leqslant l, \leqslant 11$
No. of measured reflections	2089
No. of independent reflections ($I \geqslant 2\sigma_I$)	381
No. of parameters/restraints	20/0
R_1, wR_2[a] (%) ($I > 2\sigma_I$)	5.35; 12.84
R_1, wR_2[a] (%) (all data)	6.07; 13.02
Goodness-of-fit	1.049
Extinction coefficient	0.0028(13)
Absolute structure parameter	0.10(12)
Residual electron density (e/10^6 pm^3)	4.674, −6.122

[a] $w = [\sigma^2(F_0^2) + (0.0633P)^2 + 11.13P]$ with $P = (F_o^2 + 2F_c^2)/3$.

3. Results

The powder diffraction data of $(NH_4)_3[Ta(O_2)_4]$, $Rb_3[Ta(O_2)_4]$ and $Cs_3[Ta(O_2)_4]$ are shown in Figs. 1–3 in comparison to diffraction patterns calculated on the basis of the fractional coordinates for $K_3[Ta(O_2)_4]$ from the literature [9]. The lattice constants are $a = 703.97(3)$ and $c = 861.21(6)$ pm for $(NH_4)_3[Ta(O_2)_4]$, $a = 680.00(2)$ and $c = 789.30(4)$ pm for $K_3[Ta(O_2)_4]$, $a = 706.28(2)$ and $c = 806.28(3)$ pm for $Rb_3[Ta(O_2)_4]$ and $a = 739.41(2)$ and $c = 834.30(2)$ pm for $Cs_3[Ta(O_2)_4]$.

Table 2
Final atomic coordinates, isotropic displacement parameters (10^4 pm^2), and selected atomic distances (pm) of $Rb_3[Ta(O_2)_4]$

Atom	Site	x	y	z	U_{eq}
Ta	2*a*	0	0	0	0.013(1)
Rb(2)	4*d*	0.5	0	0.75	0.028(1)
Rb(1)	2*b*	0	0	0.5	0.020(1)
O(1)	8*i*	0.1335(11)	0.1335(11)	0.1809(14)	0.023(2)
O(2)	8*i*	0.2054(10)	0.2054(10)	0.0150(50)	0.026(4)

Bond	Distance	Bond	Distance
O(1)–O(2)	153.4(0)	Rb(1)–O(2)	294.5(10)
Ta–O(1)	198.9(11)	Rb(2)–O(1)	281.2(5)
Ta–O(2)	205.5(10)	Rb(2)–O(2)	318(3)
Rb(1)–O(1)	292.4(12)	Rb(2)–O(2)	333(3)

$U_{eq} = (1/3)\sum_i \sum_j U_{ij} a_i a_j \boldsymbol{a}_i^* \boldsymbol{a}_j^*$.

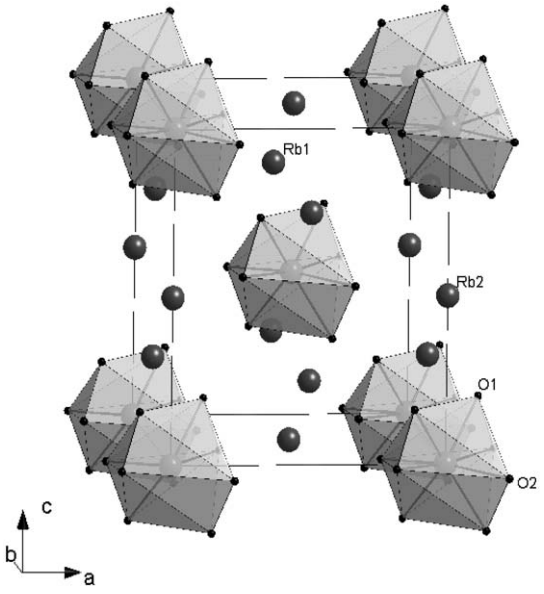

Fig. 4. Unit cell of the structure of $Rb_3[Ta(O_2)_4]$.

The structure of $Rb_3[Ta(O_2)_4]$ could be refined to $R_1 = 5.35\%$ (see Table 1). The atomic coordinates and selected atomic distances of $Rb_3[Ta(O_2)_4]$ are presented in Table 2 and the unit cell is shown in Fig. 4.

The IR- and Raman-spectra of $(NH_4)_3[Ta(O_2)_4]$, $K_3[Ta(O_2)_4]$, $Rb_3[Ta(O_2)_4]$ and $Cs_3[Ta(O_2)_4]$ are shown in Figs. 5–8.

4. Discussion

As can be seen from the good match of the experimental and the calculated powder diffraction patterns there is no doubt that $(NH_4)_3[Ta(O_2)_4]$,

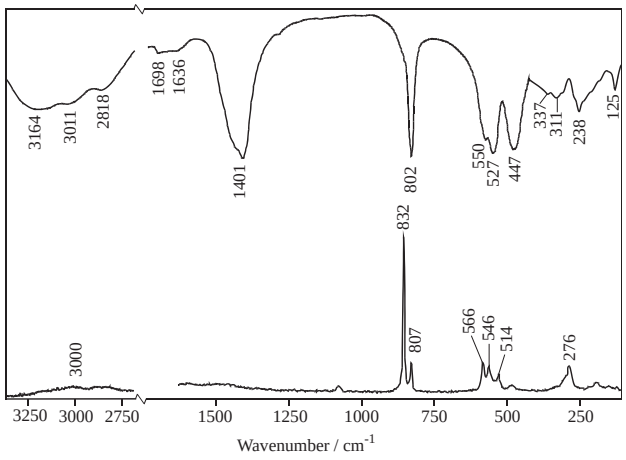

Fig. 5. IR (top) and Raman (bottom) spectra of $(NH_4)_3[Ta(O_2)_4]$.

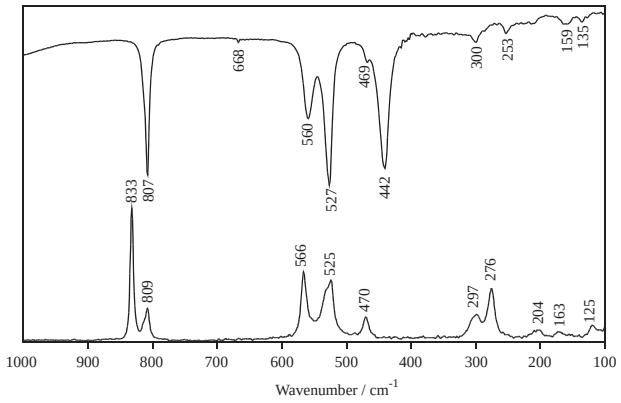

Fig. 6. IR (top) and Raman (bottom) spectra of $K_3[Ta(O_2)_4]$.

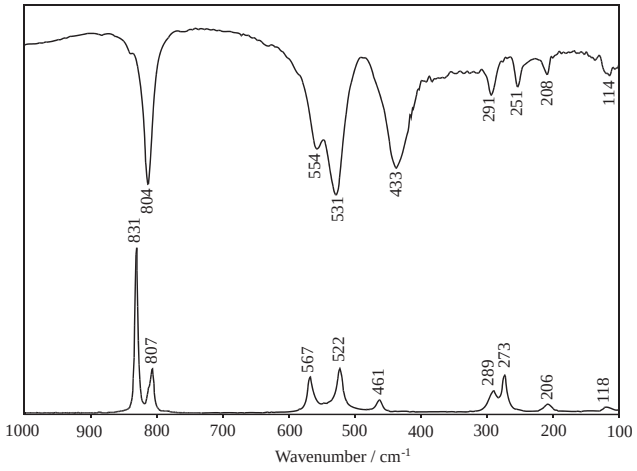

Fig. 7. IR (top) and Raman (bottom) spectra of $Rb_3[Ta(O_2)_4]$.

$K_3[Ta(O_2)_4]$, $Rb_3[Ta(O_2)_4]$ and $Cs_3[Ta(O_2)_4]$ crystallize in the $K_3[Cr(O_2)_4]$-type. In all cases the X-ray powder data could be fully indexed on the basis of the tetragonal cell.

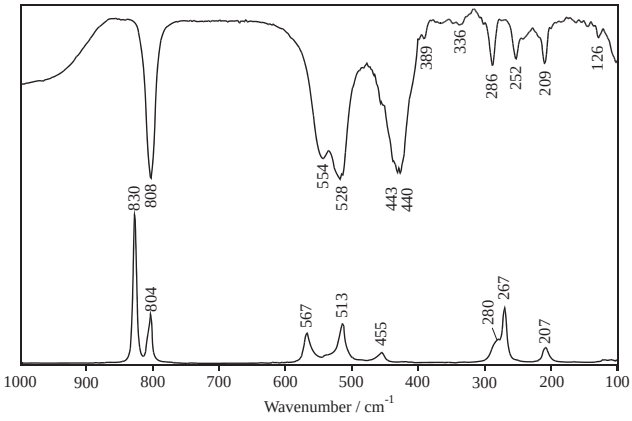

Fig. 8. IR (top) and Raman (bottom) spectra of $Cs_3[Ta(O_2)_4]$.

Table 3
Symmetry coordinates for the peroxotantalate ion $[Ta(O_2)_4]^{3-}$ (point group D_{2d}, for species E only one of the two degenerate coordinates is given)

		Symmetry coordinates
A_1	q_1	$x_1 - x_2 - x_3 + x_4 - y_1 + y_2 - y_3 + y_4$
	q_2	$z_1 + z_2 - z_3 - z_4$
	q_3	$x_5 - x_6 - x_7 + x_8 - y_5 + y_6 - y_7 + y_8$
	q_4	$z_5 + z_6 - z_7 - z_8$
A_2	q_5	$x_1 - x_2 + x_3 - x_4 + y_1 - y_2 - y_3 + y_4$
	q_6	$x_5 - x_6 + x_7 - x_8 + y_5 - y_6 - y_7 + y_8$
B_1	q_7	$x_1 - x_2 - x_3 + x_4 + y_1 - y_2 + y_3 - y_4$
	q_8	$x_5 - x_6 - x_7 + x_8 + y_5 - y_6 + y_7 - y_8$
B_2	q_9	z_{Ta}
	q_{10}	$x_1 - x_2 + x_3 - x_4 - y_1 + y_2 + y_3 - y_4$
	q_{11}	$z_1 + z_2 + z_3 + z_4$
	q_{12}	$x_5 - x_6 + x_7 - x_8 - y_5 + y_6 + y_7 - y_8$
	q_{13}	$z_5 + z_6 + z_7 + z_8$
E	q_{14}	x_{Ta}
	q_{15}	$x_1 + x_2 + x_3 + x_4$
	q_{16}	$y_1 + y_2 - y_3 - y_4$
	q_{17}	$z_1 - z_2 - z_3 + z_4$
	q_{18}	$x_5 + x_6 + x_7 + x_8$
	q_{19}	$y_5 + y_6 - y_7 - y_8$
	q_{20}	$z_5 - z_6 - z_7 + z_8$

In the structure of $Rb_3[Ta(O_2)_4]$ the peroxometallate-ion $[M(O_2)_4]^{3-}$ is of the form of a distorted dodecahedron built from 4 peroxo-groups. As in all cases known so far [7,9,18] the distance between the metal atom and the two oxygen atoms of the peroxo-group are not equal, one is slightly, i.e. 2.1 pm, longer than the other one (see Table 2). As can be seen from a comparison of the O–O distances obtained from single crystal analyses of different peroxocomplexes of $K_3[Cr(O_2)_4]$-type this distance is dependent on the central metal ion. The O–O distance increases with increasing ionic radius of the central atom from 145.2 pm for $K_3[Cr(O_2)_4]$ [7] to 150.5 pm for $Rb_3[Nb(O_2)_4]$ [18] and 151.2 pm for $K_3[Ta(O_2)_4]$ [9]. The O–O distance in H_2O_2 which is

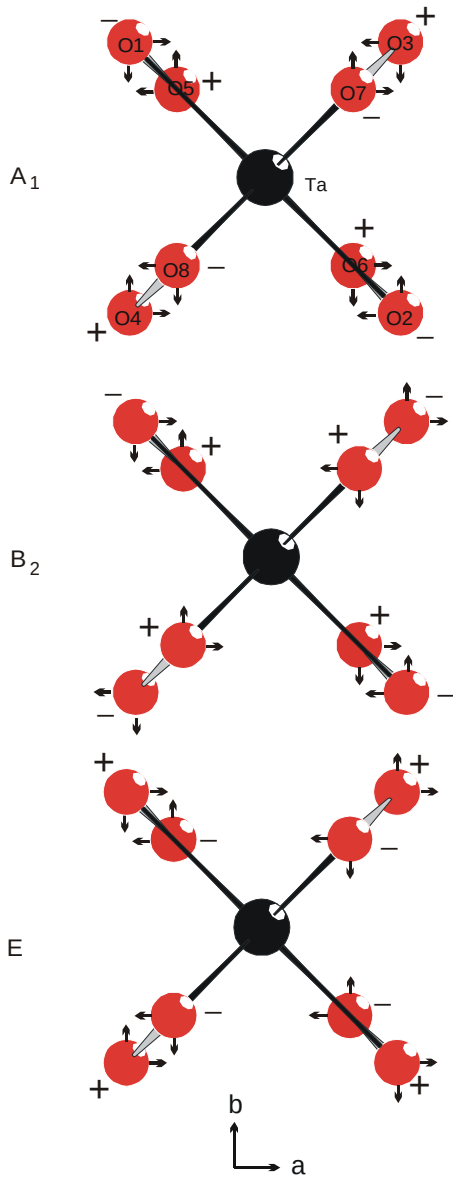

Fig. 9. Vibrational modes of the O–O stretching vibrations of the peroxometallate-anion $[M(O_2)_4]^{3-}$ (projected into the *ab*-plane, + and − designate a movement of the respective atom in the direction $+c$ or $-c$).

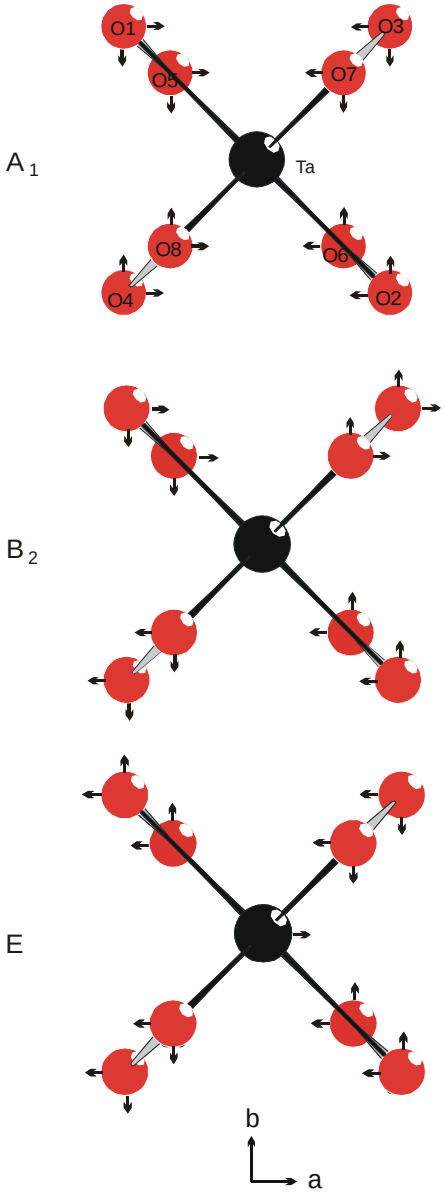

Fig. 10. Vibrational modes of the Ta–O stretching vibrations of the peroxometallate-anion $[M(O_2)_4]^{3-}$ (see Fig. 8).

147 pm in a gaseous state, is nearly identical to the one of the peroxochromate.

The factor group analysis for the $K_3[Cr(O_2)_4]$ type results in the following distribution of the vibrational degrees of freedom over the species of point group D_{2d} [15,18]:

$$\Gamma = 4A_1(\mathrm{Ra}) + 2A_2 + 3B_1(\mathrm{Ra}) + 6B_2(\mathrm{IR},\mathrm{Ra}) + 9E(\mathrm{IR};\mathrm{Ra}).$$

Symmetry coordinates for the $[Ta(O_2)_4]^{3-}$ ion based on a cartesian coordinate system with $x||a$, $y||b$, and $z||c$ (see Fig. 4) are given in Table 3.

The stretching vibrations of the peroxo-groups which according to the site group analysis of the $[Ta(O_2)_4]^{3-}$ ion (site group symmetry D_{2d}) [15] belong to the species A_1, B_2 and E are observed in the region with $\tilde{\nu} > 800\,\mathrm{cm}^{-1}$ (see Figs. 5–8). Vibrational modes for the three stretching vibrations of the peroxo-groups can be derived from the symmetry coordinates given in Table 3 by the following linear combinations: A_1: $(q_1 - q_2 - q_3 + q_4)$; B_2: $(-q_{10} - q_{11} + q_{12} + q_{13})$; E: $(q_{15} - q_{16} + q_{17} - q_{18} + q_{19} - q_{20})$ which are shown in Fig. 8. As can be seen from the figure the tantalum atoms do not take part in all these vibrations but due to the real contribution of the different symmetry coordinates to

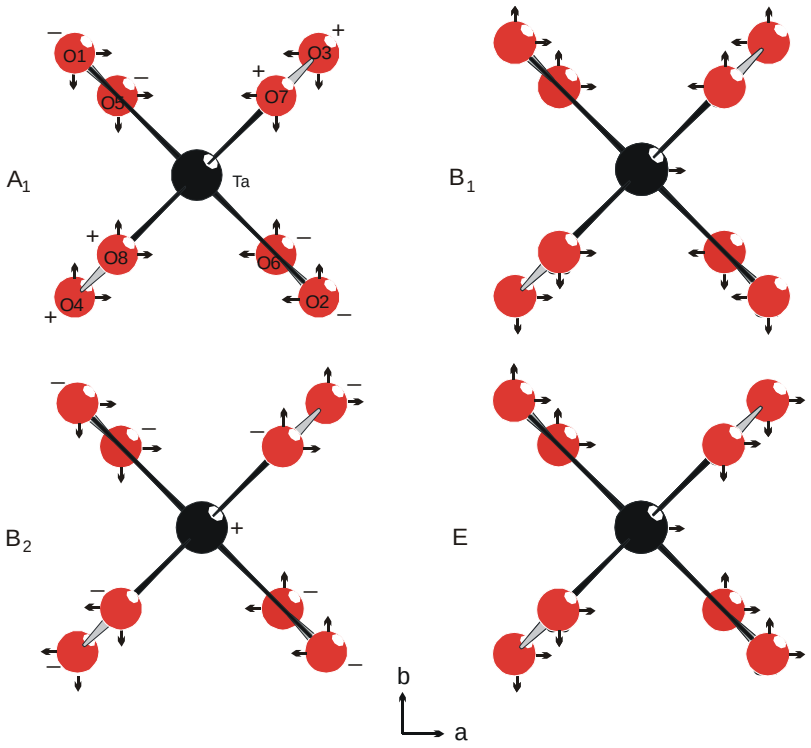

Fig. 11. Vibrational modes of the Ta–O bending vibrations of the peroxometallate-anion $[M(O_2)_4]^{3-}$ (see Fig. 8).

the normal modes, which can only be evaluated by a detailed force constant calculation, there may be some mixing of the O–O with Ta–O stretching vibrations.

The strong lines in the Raman spectra at 830–833 cm^{-1} are due to the total symmetric vibration of species A_1 where all 4 peroxo-groups vibrate in phase. The strong bands in the IR spectra at 802–808 cm^{-1} which are also observed in the Raman spectra as weak lines with slightly different values due to the accuracy of the measurements are assigned to the vibrations of species E. The third vibration of the peroxo-groups of species B_2 is not observed in both the Raman and the IR spectra, though IR as well as Raman active.

As in the case of the corresponding peroxochromates [15] the vibrations of the peroxo-groups are nearly not affected by the different cations. From that we concluded in the case of the peroxochromates $A_3[Cr(O_2)_4]$ with $A = NH_4^+$, K and Rb [15] that the O–O distances in these three compounds should be equal or at least very similar. But a comparison of the O–O distances obtained from single crystal data shows that in the case of the tantalates the O–O distances change from 151.2 pm for the potassium compound [9] to 153.4 pm for the rubidium compound (see Table 2) whereby the total symmetric vibration of the peroxo-groups of species A_1 shifts by 2 cm^{-1} only (see Figs. 5 and 8). Comparing $K_3[Cr(O_2)_4]$ to $K_3[Ta(O_2)_4]$ on the other side one finds that the lengthening of the O–O distance by 6 pm is accompanied by a relatively much higher shift of the same O–O mode by 86 cm^{-1}. These large differences in the shift of the O–O stretching frequencies with a change in the O–O distance are surely caused by a different degree of coupling of the O–O and Ta–O stretching modes in the peroxochromates and -tantalates which seems to be stronger in the case of the tantalates. Thus, the vibrational frequencies of this mode can not be used as a direct measure for the O–O distances in these compounds.

The small shift to lower wavenumbers with increasing mass of the alkali metal atoms must be due to slight changes in the O–O stretching force constants due to some minor interaction of these cations with the O_2^{2-} ligands by which the electron density in the π^*-orbitals of the peroxo-groups is reduced, thus strengthening the O–O bond (Fig. 9).

The three Ta–O stretching vibrations of the peroxo-tantalate ion belonging to the species A_1, B_2 and E are observed in the region $600\,cm^{-1} > \tilde{\nu} > 500\,cm^{-1}$. Vibrational modes of these vibrations derived from the symmetry coordinates by the linear combinations A_1: $(q_1 + q_3)$; B_2: $(q_{10} + q_{12})$; E: $(q_{14} - q_{15} + q_{16} - q_{18} + q_{19})$ are shown in Fig. 10. From this picture it is obvious that only in the case of the E mode the central atom of the peroxocomplex takes part in the vibration thus causing the shift of one of the M–O stretching vibrations from 676 cm^{-1} in $K_3[Cr(O_2)_4]$ [15] via 596 cm^{-1} for $Rb_3[Nb(O_2)_4]$ [18] to 550–560 cm^{-1} in the tantalum compounds.

The bending vibrations of the peroxotantalate ion which are observed in the range $500\,cm^{-1} > \tilde{\nu} > 200\,cm^{-1}$ can be derived from the corresponding vibrations of a tetrahedron with rigid O_2-units at the corners. The vibrational modes as obtained from the symmetry coordinates of Table 3 are shown in Fig. 11. The vibrations of species A_1 and B_1 correspond to the symmetrical bending vibration of a tetrahedron and those of species B_2 and E to the asymmetrical bending vibration. A major participation of the central atom we only expect for the bending vibration of species B_2 which should be combined with a strong change in dipole moment and thus give rise to a strong absorption. As can be seen from the spectra there is one strong band in the respective region of the spectrum at $442\,cm^{-1}$ for $K_3[Ta(O_2)_4]$ but this absorption is shifted to lower wavenumbers when the central atom is replaced by a lighter one, as can be seen from a comparison with $K_3[Nb(O_2)_4]$ [19] and $K_3[Cr(O_2)_4]$ [15] where this band is found at 435 and $426\,cm^{-1}$, respectively. This unusual shift to higher wavenumbers with growing mass of the central atom may be caused by a growing mode mixing of the bending with the O–O stretching vibrations which already has been discussed for the O–O stretching vibrations (see above) and which could overcompensate the mass effect.

The translational lattice vibrations and the librations of the $[Ta(O_2)_4]^{3-}$ ion will occur below $200\,cm^{-1}$. An assignment of the translational and librational lattice modes of the peroxochromate-ions is not possible, as the spectra are not well resolved in the low wavenumber region.

In the case of the ammonium compound additional to the vibrations of the $K_3[Ta(O_2)_4]$-type the internal vibrations of the ammonium ions which are observed above $1400\,cm^{-1}$ (see Fig. 5). Librational modes of the ammonium ion which may be found below $1000\,cm^{-1}$ are not clearly identified in the spectrum.

5. Conclusion

According to X-ray single crystal and powder diffraction data we could show that all the peroxotantalates $A_3[Ta(O_2)_4]$ with $A = NH_4^+$, K, Rb, Cs crystallize in the $K_3[Cr(O_2)_4]$-type. The stretching vibrations of the peroxo-groups are nearly not affected by the A cations, they are found in the range 830–$833\,cm^{-1}$ for the Raman active vibration of species A_1 and 804–$808\,cm^{-1}$ for the strong IR absorption peak of species E. Both vibrations are not a direct measure for the O–O bond length due to some coupling with the Ta–O stretching vibrations. Only one of the Ta–O stretching vibrations which belongs to species E shows a major influence of the central atom of the peroxocomplex as it involves a motion of the central atom while all other vibrations of this type are solely translational motions of the rigid O_2^{2-} units as can be seen from the vibrational modes derived from the symmetry coordinates of the $[Ta(O_2)_4]^{3-}$ ion.

References

[1] E.H. Riesenfeld, H.E. Wohlers, W.A. Kutsch, Chem. Ber. (1905) 1885.
[2] I.A. Wilson, Ark. Kemi 15B (1941) 1.
[3] R. Stomberg, C. Brosset, Acta Chem. Scand. 14 (1960) 441.
[4] R. Stomberg, Acta Chem. Scand. 17 (1963) 1563.
[5] J.D. Swalen, J.A. Ibers, J. Chem. Phys. 37 (1962) 17.
[6] J. Fischer, A. Veillard, R. Weiss, Theor. Chim. Acta 24 (1972) 317.
[7] R.M. Wood, K.A. Abboud, R.C. Palenik, G.J. Palenik, Inorg. Chem. 39 (2000) 2065.
[8] B. Cage, N.S. Dalal, Chem. Mater. 13 (2001) 880.
[9] G. Wehrum, R. Hoppe, Z. Anorg. Allg. Chem. 619 (1993) 1315.
[10] K.I. Selezneva, L.A. Nisel'son, Russ. J. Inorg. Chem. 13 (1968) 45.
[11] W.P. Griffith, J. Chem. Soc. (1964) 5248.
[12] W.P. Griffith, T.D. Wickins, J. Chem. Soc. (A) (1968) 397.
[13] G.V. Jere, L. Surendra, M.K. Gupta, Thermochim. Acta 63 (1983) 229.
[14] G.A. Bogdanov, G.K. Yurchenko, O.V. Popov, Zh. Neorg. Khim. 27 (1982) 2143.
[15] H. Haeuseler, G. Haxhillazi, J. Raman Spectrosc. 34 (2003) 339.
[16] WinXpow Version 1.04, Stoe Power Diffraction Software, Stoe&CIE GmbH, Darmstadt, 1999.
[17] G.M. Sheldrik, SHELX-97 program for the crystal structure refinement, University Göttingen, 1997.
[18] H. Haeuseler, M. Wagener, H. Müller, Z. Naturforsch. 52b (1997) 1082.
[19] G. Haxhillazi, Ph.D. Thesis, University of Siegen, 2003.